Supporting Information

Ultrathin 2D Metal-Organic-Frameworks (Nanosheets and Nanofilms) Based xD-2D Hybrid Nanostructures as Biomimetic Enzymes and Supercapacitors

Wu-Shuang Bai*,Si-Jia Li, Jun-Ping Ma, Wei Cao, Jian-Bin Zheng*

Experimental Section

Chemicals. Nickel nitrate hexahydrate ($Ni(NO_3)_2 \cdot 6H_2O$), cobalt nitrate hexahydrate ($Co(NO_3)_2 \cdot 6H_2O$), copper nitrate trihydrate ($Cu(NO_3)_2 \cdot 3H_2O$), polyvinylpyrrolidone (PVP, MW=40,000g/mol), tetrakis(4-carboxyphenyl)porphyrin (TCPP), N,N-diethylformamide (DEF), N,N-dimethylformamide (DMF), catalase, ascorbic acid (AA, AR), uric acid (UA) and glucose (Glu) were purchased from Sigma-Aldrich. Ethanol (99.9%) and H_2O_2 (30%, v/v aqueous solution) were purchased from Tianli Chemistry Reagent Co., Ltd (Tianjin, China). All the materials were used as received without further purification. All used solutions were prepared in Milli-Q water (18.2 MΩ·cm, Milli-Q System, Millipore, USA).

Characterizations. SEM images were obtained using a field emission scanning electron microscope (SU8020 HITACHI Japan). A transmission electron microscope (Tecnai G^2 F20 S-TWIN, FEI, USA) coupled with energy dispersive X-ray spectroscopy (EDS) was used to take the TEM images and EDS elemental mappings. X-ray diffraction (XRD) patterns were recorded with a X-ray diffractometer (D/MAX-3C, Rigaku Japan). A Dimension 3100 AFM with Nanoscope IIIa controller (Veeco, Fremont, CA) was used to record AFM images in tapping mode under ambient conditions. Fourier transform infrared spectroscopy (FTIR) was recorded with TENSIR 27 (Bruker, German). X-ray photoelectron spectroscopy (XPS) was recorded on a VG ESCALAB 220i-XL instrument. All the electrochemical measurements were carried out on a CHI 660E electrochemical workstation (Shanghai CH Instrument Co. Ltd., China).

Synthesis of Cu-TCPP nanofilm. First, 5.0 mg of $Cu(NO_3)_2 \cdot 3H_2O$, and 20.0 mg of PVP were dissolved in 16 mL of the mixture of DMF and ethanol (V:V = 3:1) in a 25 mL capped beaker. Then, the obtained solution was mixed with 12 mg of TCPP and further ultrasonicated for 10 min. At last, the solution was transferred into a 20 mL Teflon-lined stainless steel autoclave and the reaction was performed under 80°C for 3 h, and then cooled down to room temperature. The resulting colloidal products were collected by centrifugation and washed 3 times with an ethanol.

Synthesis of Co-TCPP nanofilm. First, 15.0 mg of $Co(NO_3)_2 \cdot 6H_2O$, and 20.0 mg of PVP were dissolved in 16 mL of the mixture of DMF and ethanol (V:V = 3:1) in a 25 mL capped beaker. Then, the obtained solution was mixed with 12 mg of TCPP and further ultrasonicated for 10 min. At last, the solution was transferred into a 20 mL Teflon-lined stainless steel autoclave and the reaction was performed under 80°C for 24 h, and then cooled down to room temperature. The resulting colloidal products were collected by centrifugation and washed 3 times with an ethanol.

Synthesis of Ni-TCPP nanofilm. First, 15.0 mg of $Ni(NO_3)_2 \cdot 6H_2O$, and 20.0 mg of PVP were dissolved in 16 mL of the mixture of DMF and ethanol (V:V = 3:1) in a 25 mL capped beaker. Then, the obtained solution was mixed with 12 mg of TCPP and further ultrasonicated for 10 min. At last, the solution was transferred into a 20 mL Teflon-lined stainless steel autoclave and the reaction was performed under 80°C for 24 h, and then cooled down to room temperature. The resulting colloidal products were collected by centrifugation and washed 3 times with an ethanol.

Synthesis of Cu-TCPP nanosheet. First, 5.0 mg of $Cu(NO_3)_2 \cdot 3H_2O$ were dissolved in 16 mL of the mixture of DEF and ethanol (V:V = 3:1) in a 25 mL capped beaker. Then, the obtained solution was mixed with 12 mg of TCPP and further ultrasonicated for 10 min. At last, the solution was transferred into a 20 mL Teflon-lined stainless steel autoclave and the reaction was performed under 80°C for 3 h, and then cooled down to room temperature. The resulting colloidal products were collected by centrifugation and washed 3 times with an ethanol.

Synthesis of Co-TCPP nanosheet. First, 15.0 mg of $Co(NO_3)_2 \cdot 6H_2O$ were dissolved in 16 mL of the mixture of DEF and ethanol (V:V = 3:1) in a 25 mL capped beaker.

Then, the obtained solution was mixed with 12 mg of TCPP and further ultrasonicated for 10 min. At last, the solution was transferred into a 20 mL Teflon-lined stainless steel autoclave and the reaction was performed under 80°C for 24 h, and then cooled down to room temperature. The resulting colloidal products were collected by centrifugation and washed 3 times with an ethanol.

Synthesis of Ni-TCPP nanosheet. First, 15.0 mg of $Ni(NO_3)_2 \cdot 6H_2O$ were dissolved in 16 mL of the mixture of DEF and ethanol (V:V = 3:1) in a 25 mL capped beaker. Then, the obtained solution was mixed with 12 mg of TCPP and further ultrasonicated for 10 min. At last, the solution was transferred into a 20 mL Teflon-lined stainless steel autoclave and the reaction was performed under 80°C for 24 h, and then cooled down to room temperature. The resulting colloidal products were collected by centrifugation and washed 3 times with an ethanol.

Synthesis of M-TCPP nanofilm/CNT. Synthesis of M-TCPP nanofilm/CNT was similar to that of corresponding M-TCPP nanofilm except for addition of 5 mg CNT. In brief, CNT, corresponding nitrate and PVP were dissolved in the mixture of DMF and ethanol (V:V = 3:1). Then, the obtained solution was mixed with TCPP and further ultrasonicated for 15 min. At last, the solution was transferred into a 20 mL Teflon-lined stainless steel autoclave and the reaction was performed under corresponding situation, and then cooled down to room temperature. The resulting colloidal products were collected by centrifugation and washed 3 times with an ethanol.

Synthesis of M-TCPP nanosheet/GO. Synthesis of M-TCPP nanosheet/GO was similar to that of corresponding M-TCPP nanosheet except for addition of 5 mg GO. In brief, GO and corresponding nitrate were dissolved in the mixture of DEF and ethanol (V:V = 3:1). Then, the obtained solution was mixed with TCPP and further ultrasonicated for 15 min. At last, the solution was transferred into a 20 mL Teflon-lined stainless steel autoclave and the reaction was performed under corresponding situation, and then cooled down to room temperature. The resulting colloidal products were collected by centrifugation and washed 3 times with an ethanol.

Electrochemical measurement. The electrochemical cell with conventional three-

electrode setup, i.e. a saturated calomel electrode or Ag/AgCl reference electrode, a Pt wire auxiliary electrode, and the prepared working electrode, was used for the electrochemical test. Prior to use, all the glassy carbon electrodes (GCE) were polished with alumina slurry and then sonicated for 5 min in ethanol and deionized water, respectively.

For sensing application, 0.1 M PBS (pH 7.2) was used as electrolyte, saturated calomel electrode was used as reference electrode, and the electrolyte was purged with N_2 for at least 15 min to remove oxygen prior to electrochemical measurements. The working electrodes were prepared by Langmuir-Schäfer method. In brief, the synthesized materials were first dispersed in ethanol to obtain a colloidal suspension with a concentration of 1.0 mg mL^{-1}. Then the suspension was gently dropped onto the surface of water in a beaker. After the materials spontaneously spread to form a thin film on water, the film was transferred onto GCE. Finally, the film-coated GCE was immersed into fresh water to remove the loosely deposited materials. The aforementioned procedure is defined as one deposition cycle. By repeating the aforementioned deposition procedure, materials/GCE (n) (n = number of deposition cycle) could be obtained.

For supercapacitor application, Ag/AgCl reference electrode was used. The working electrode was prepared as the reference.[S1] In brief, 1 mg materials were dispersed in 1 mL EtOH by sonication for half an hour, to form a stable suspension. Then, 5 μL of this suspension was drop cast onto the working area of GCEs and dried under infrared lamp irradiation and subsequently the GCE was covered with a smooth layer of Nafion. After drying, the modified GCEs were immersed into fresh water to remove the loosely deposited materials. 1M H_2SO_4 was used as electrolyte for Cu-TCPP MOF modified electrode while 6 M KOH was used for Co and Ni MOF modified electrodes.

Real-time tracking of H_2O_2 in living cells. PC-12 rat adrenal medulla pheochromocytoma cells were provided by Xi'an Medical University (Xi'an, Shaanxi, PR China). The cells were cultured in Dulbecco's modified Eagle's medium (DMEM). The medium was supplemented with 100 units mL^{-1} of penicillin, 100 units mL^{-1} of

streptomycin and 10% bovine serum. The culture was incubated under 37°C. To utilize the cells for electrochemical measurements, the cells were separated from the culture by centrifugation at 1300 rpm and washed three times with sterile buffer to remove any remaining culture medium or serum and suspended in PBS (0.1 M). Cell number was about 4×10^7 which was estimated by a cell counter and the cell solution was 5mL. 1 μM AA was injected to the cells suspension every time to motivate cells generate H_2O_2. The catalase was 300U/mL. The electrochemical experiments were conducted in water bath under 37°C.

References

S1. M. Saraf, R. Rajakb, S. M. Mobin, J. Mater. Chem. A, 2016, 4, 16432–16445

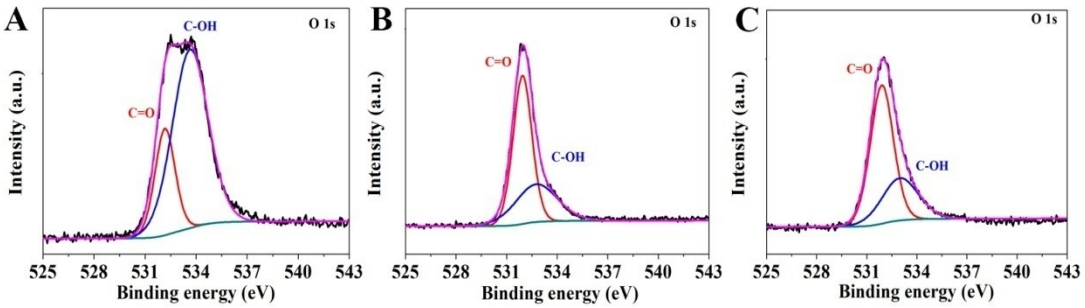

Figure S1. High-resolution O XPS spectra of TCPP (A), 2D Cu-TCPP nanofilm (B) and 2D Cu-TCPP nanosheet (C).

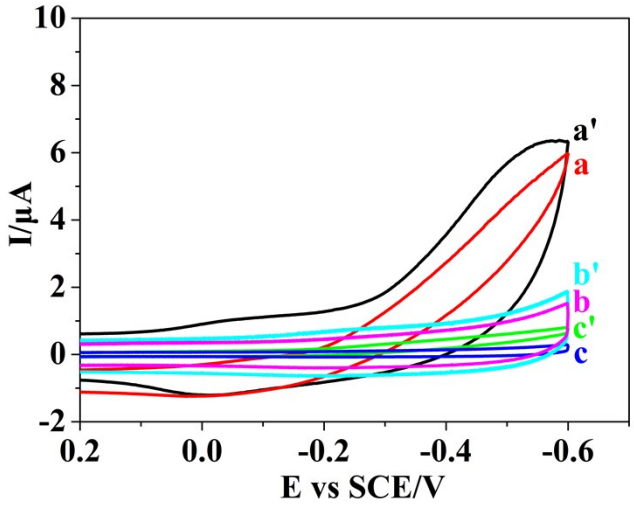

Figure S2. CV curves of GO/GCE (a, a'), CNT/GCE (b, b') and bare GCE (c, c')in absence (a, b and c) and presence (a', b' and c') of 0.2 mM H_2O_2 in PBS (0.1 M, pH

7.2).

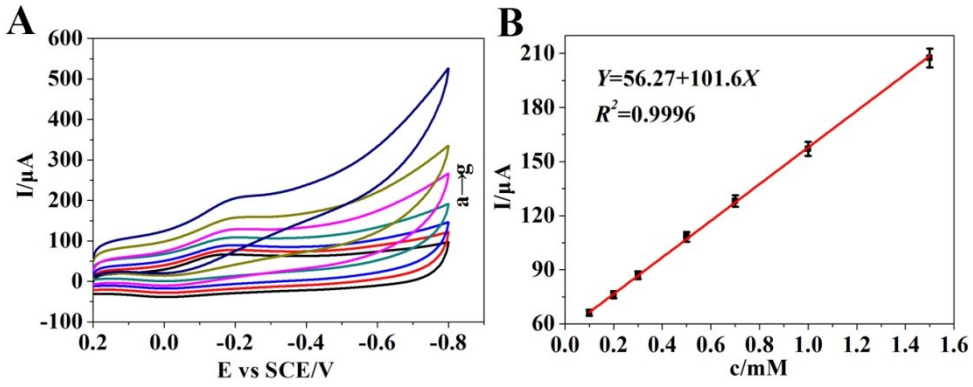

Figure S3. (A) CV curves of Cu-TCPP nanofilm/CNT/GCE in 0.1M PBS (pH 7.2) in presence of H_2O_2 with different concentrations (from a to g: 0.1, 0.2, 0.3, 0.5, 0.7, 1.0 and 1.5mM) at a scan rate of 50mV/s. (B) The corresponding linear fitting programs of Cu-TCPP/CNT/GCE between peak current and H_2O_2concentration.

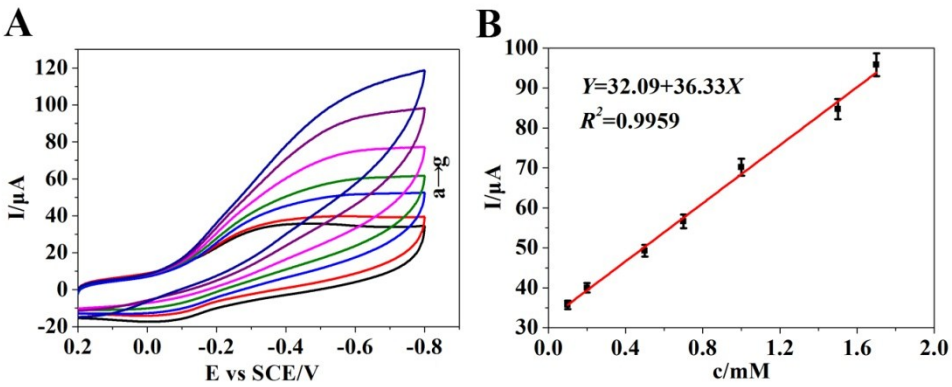

Figure S4. (A) CV curves of Co-TCPP nanofilm/CNT/GCE in 0.1M PBS (pH 7.2) in presence of H_2O_2 with different concentrations (from a to g: 0.1 to 1.7mM) at a scan rate of 50mV/s. (B) The corresponding linear fitting programs of Co-TCPP nanofilm/CNT/GCE between peak current and H_2O_2 concentration.

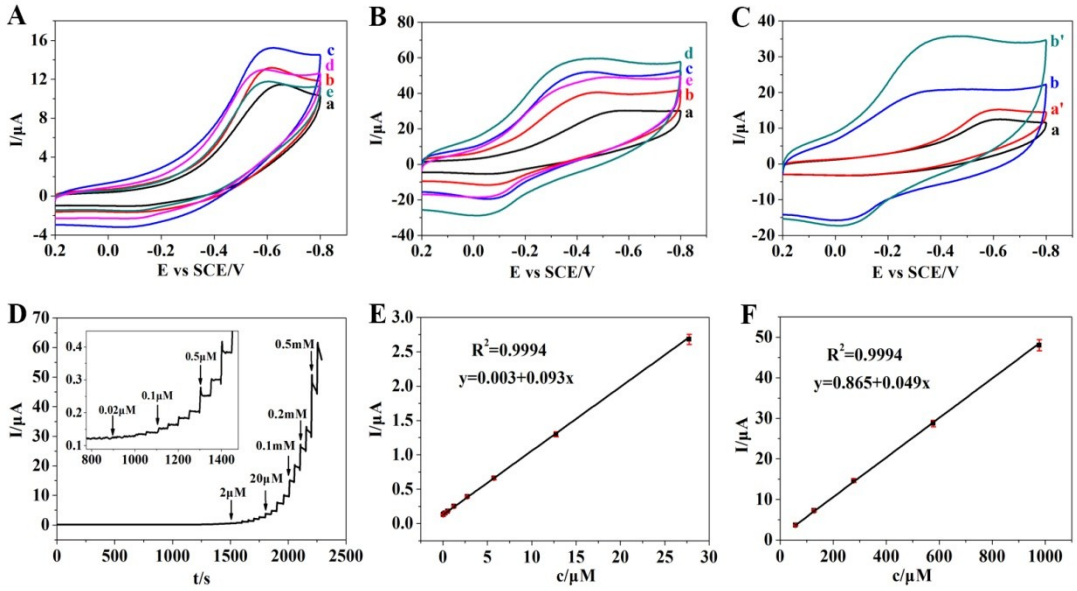

Figure S5. (A, B) CV curves of Co-TCPP nanofilm/GCE (A) and Co-TCPP nanofilm/CNT/GCE (B) in 0.1M PBS (pH 7.2) in presence of 0.2mM H_2O_2 at a scan rate of 50mV/s (a-e: n=1, 2, 3, 4 and 5). (C) CV curves of Co-TCPP nanofilm/GCE (n=3) (a, a')and Co-TCPP nanofilm/CNT/GCE(n=4) (b, b') in 0.1M PBS (pH 7.2) in absence (a, b) and presence (a', b') of 0.2mM H_2O_2 at a scan rate of 50mV/s. (D) Typical amperometric responses of Co-TCPP nanofilm/CNT/GCE(n=4) with successive injection of H_2O_2 in PBS (0.1 M, pH 7.2) under -0.45 V. (E, F) The corresponding linear fitting programs of Co-TCPP nanofilm/CNT/GCE(n=4) between peak current and H_2O_2 concentration.

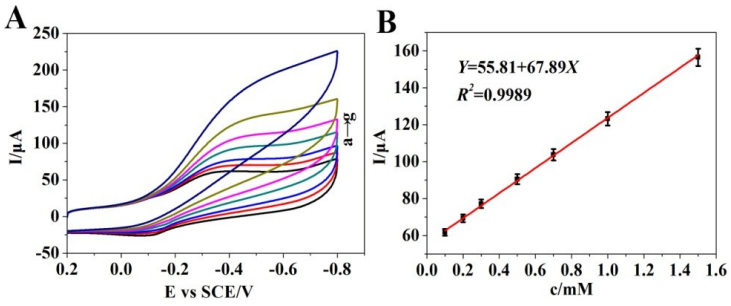

Figure S6. (A) CV curves of Ni-TCPP nanofilm/CNT/GCE in 0.1M PBS (pH 7.2) in presence of H_2O_2 with different concentrations (from a to g: 0.1 to 1.5mM) at a scan rate of 50mV/s. (B) The corresponding linear fitting programs of Ni-TCPP nanofilm/CNT/GCE between peak current and H_2O_2 concentration.

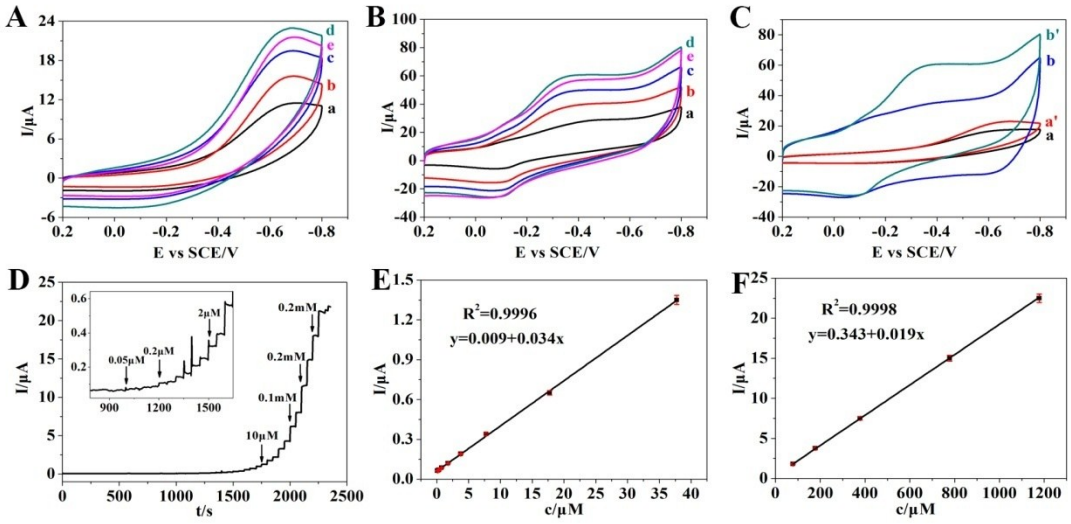

Figure S7. (A, B) CV curves of Ni-TCPP nanofilm/GCE (A) and Ni-TCPP nanofilm/CNT/GCE (B) in 0.1M PBS (pH 7.2) in presence of 0.2mM H_2O_2 at a scan rate of 50mV/s (a-e: n=1, 2, 3, 4 and 5). (C) CVcurves of Ni-TCPP nanofilm/GCE (n=4) (a, a') and Ni-TCPP nanofilm/CNT/GCE(n=4) (b, b') in 0.1M PBS (pH 7.2) in absence (a, b) and presence (a', b') of 0.2mM H_2O_2 at a scan rate of 50mV/s. (D) Typical amperometric responses of Ni-TCPP nanofilm/CNT/GCE(n=4) with successive injection of H_2O_2 in PBS (0.1 M, pH 7.2) under -0.4 V. (E, F) The corresponding linear fitting programs of Ni-TCPP nanofilm/CNT/GCE(n=4) between peak current and H_2O_2 concentration.

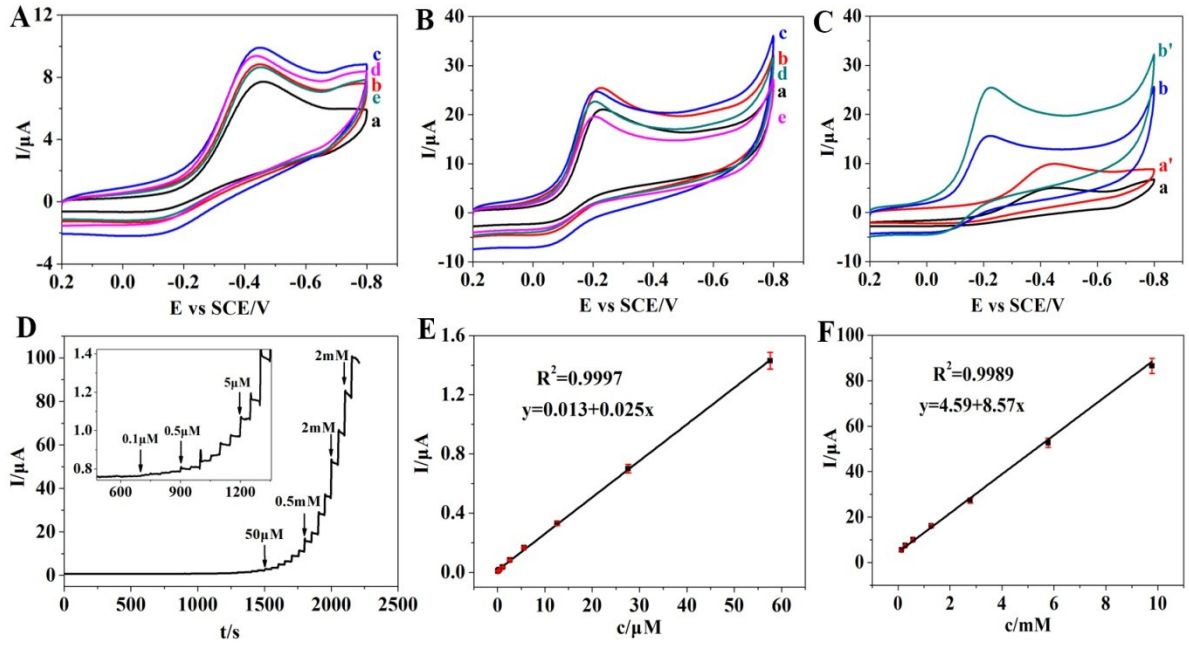

Figure S8. (A, B) CV curves of Cu-TCPP nanosheet/GCE (A) and Cu-TCPP nanosheet/GO/GCE (B) in 0.1M PBS (pH 7.2) in presence of 0.2mM H_2O_2 at a scan rate of 50 mV/s (a-e: n=1, 2, 3, 4 and 5). (C) CV curves of Cu-TCPP nanosheet/GCE (n=3) (a, a') and Cu-TCPP nanosheet/GO/GCE (n=3) (b, b') in 0.1M PBS (pH 7.2) in absence (a, b) and presence (a', b') of 0.2mM H_2O_2 at a scan rate of 50 mV/s. (D) Typical amperometric responses of Cu-TCPP nanosheet/GO/GCE (n=3) with successive injection of H_2O_2 in PBS (0.1 M, pH 7.2) under -0.2 V. (E, F) The corresponding linear fitting programs of Cu-TCPP nanosheet/GO/GCE (n=3) between peak current and H_2O_2 concentration.

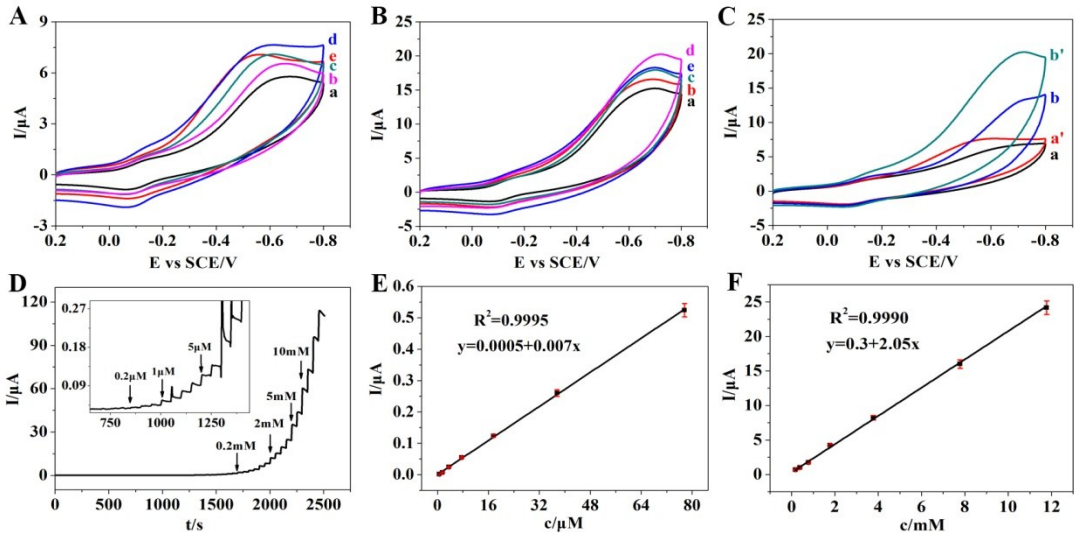

Figure S9. (A, B) CV curves of Co-TCPP nanosheet/GCE(A) and Co-TCPP nanosheet/GO/GCE (B) in 0.1M PBS (pH 7.2) in presence of 0.2mM H_2O_2 at a scan rate of 50mV/s (a-e: n=1, 2, 3, 4 and 5). (C) CVcurves of Co-TCPP nanosheet/GCE (n=4) (a, a')and Co-TCPP nanosheet/GO/GCE (n=4) (b, b') in 0.1M PBS (pH 7.2) in absence (a, b) and presence (a', b') of 0.2mM H_2O_2 at a scan rate of 50mV/s. (D) Typical amperometric responses of Co-TCPP nanosheet/GO/GCE (n=4) with successive injection of H_2O_2 in PBS (0.1 M, pH 7.2) under -0.7 V. (E, F) The corresponding linear fitting programs of Co-TCPP nanosheet/GO/GCE(n=4) between peak current and H_2O_2 concentration.

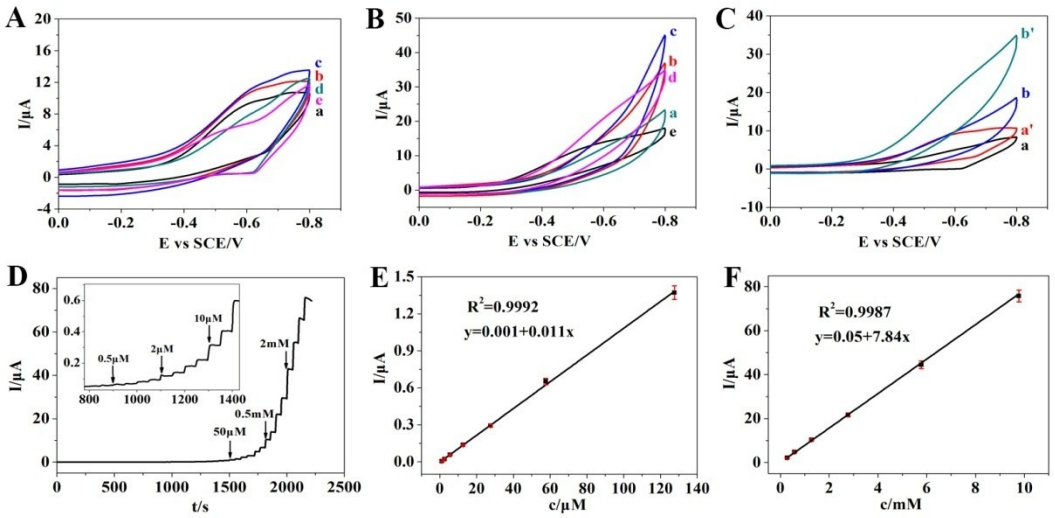

Figure S10. (A, B) CV curves of Ni-TCPP nanosheet/GCE(A) and Ni-TCPP nanosheet/CNT/GCE (B) in 0.1M PBS (pH 7.2) in presence of 0.2mM H_2O_2 at a scan rate of 50mV/s (a-e: n=1, 2, 3, 4 and 5). (C) CVcurves of Ni-TCPP nanosheet/GCE (n=3) (a, a')and Ni-TCPP nanosheet/CNT/GCE(n=3) (b, b') in 0.1M PBS (pH 7.2) in absence (a, b) and presence (a', b') of 0.2mM H_2O_2 at a scan rate of 50mV/s. (D) Typical amperometric responses of Ni-TCPP nanosheet/CNT/GCE(n=3) with successive injection of H_2O_2 in PBS (0.1 M, pH 7.2) under -0.6 V. (E, F) The corresponding linear fitting programs of Ni-TCPP nanosheet/CNT/GCE(n=3) between peak current and H_2O_2 concentration.

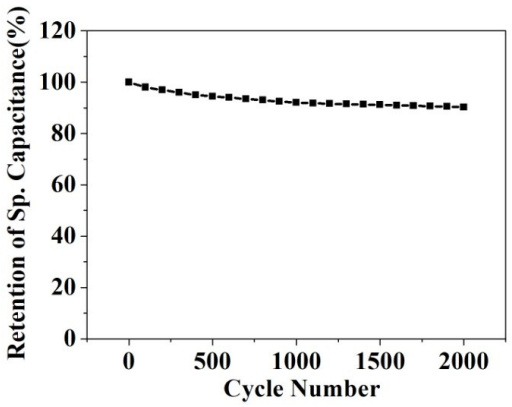

Figure S11. Long-term cycling performance of the Ni-TCPP nanofilm/CNT/GCE at the current density of 5A/g.

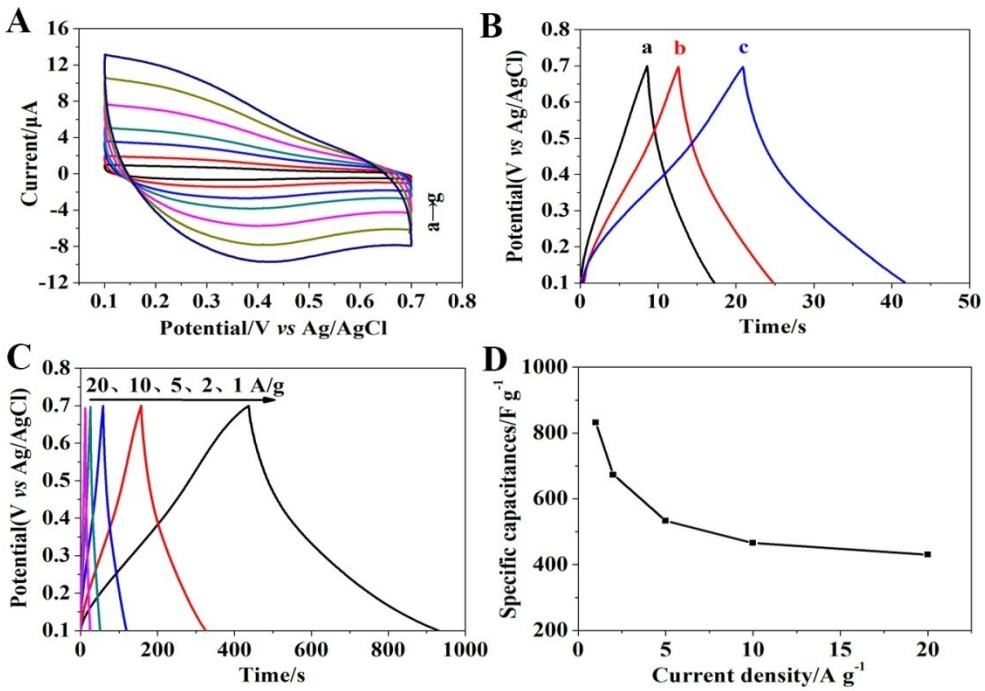

Figure S12. (A) CV curves of Cu-TCPP nanofilm/CNT/GCE at di□erent scan rates (a-g: 10-200 mV/s). (B) GCD curves of CNT/GCE (a), Cu-TCPP nanofilm/GCE (b) and Cu-TCPP nanofilm/CNT/GCE (c) at a current density of 10A/g. (C) GCD curves of Cu-TCPP nanofilm/CNT/GCE at different current densities (1-20A/g). (D) Specific capacitances derived from the GCE curves at the current density of 1-20 A/g.

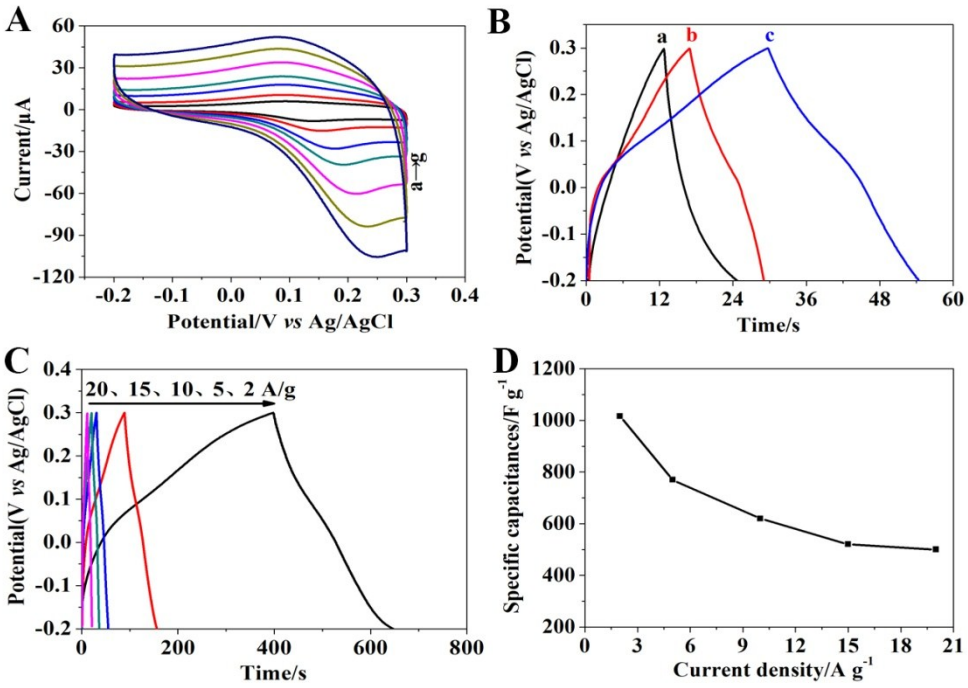

Figure S13. (A) CV curves of Co-TCPP nanofilm/CNT/GCE at di□erent scan rates (a-g: 10-200 mV/s). (B) GCD curves of CNT/GCE (a), Co-TCPP nanofilm/GCE (b) and Co-TCPP nanofilm/CNT/GCE (c) at a current density of 10A/g. (C) GCD curves of Co-TCPP nanofilm/CNT/GCE at different current densities (2-20A/g). (D) Specific capacitances derived from the GCE curves at the current density of 2-20 A/g.

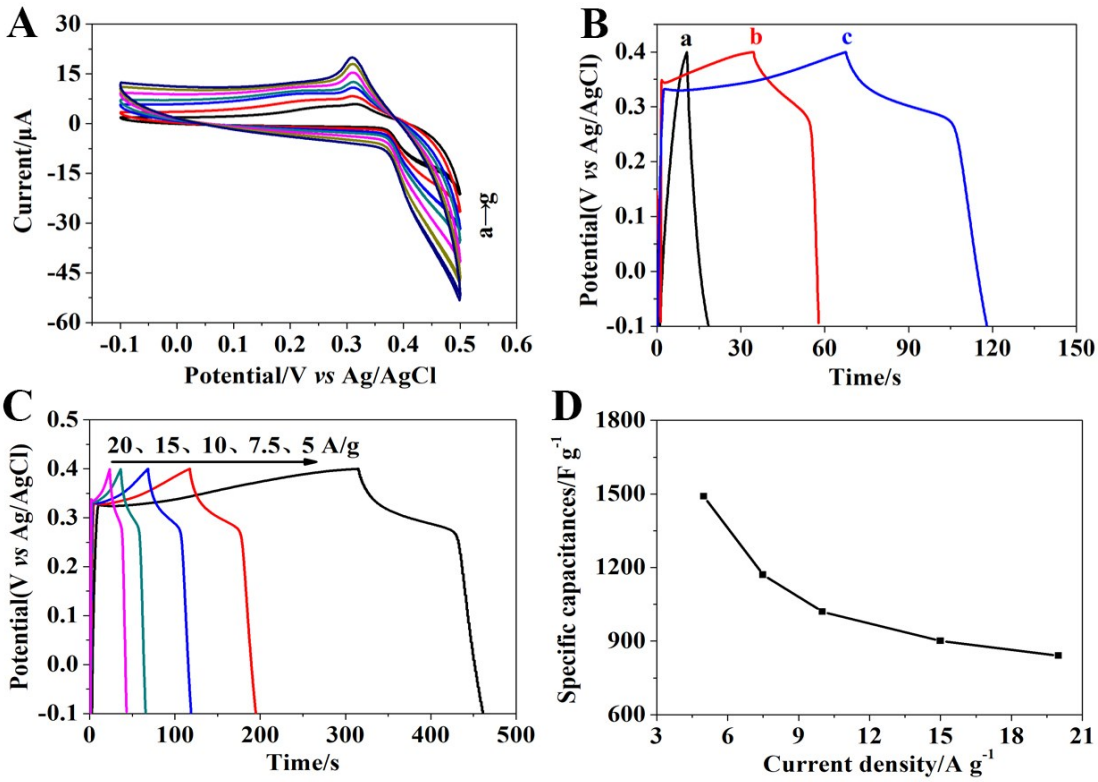

Figure S14. (A) CV curves of Ni-TCPP nanosheet/GO/GCE at di□erent scan rates (a-g: 10-200 mV/s). (B) GCD curves of GO/GCE (a), Ni-TCPP nanosheet/GCE (b) and Ni-TCPP nanosheet/GO/GCE (c) at a current density of 10A/g. (C) GCD curves of Ni-TCPP nanosheet/GO/GCE at different current densities (5-20A/g). (D) Specific capacitances derived from the GCE curves at the current density of 5-20 A/g.

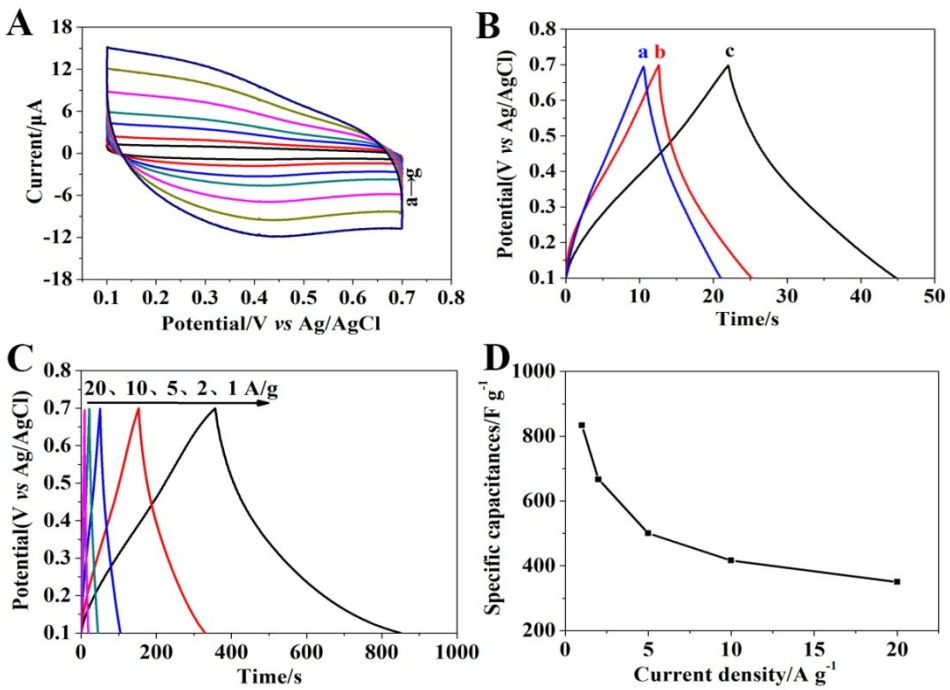

Figure S15. (A) CV curves of Cu-TCPP nanosheet/GO/GCE at di□erent scan rates (a-g: 10-200 mV/s). (B) GCD curves of GO/GCE (a), Cu-TCPP nanosheet/GCE (b) and Cu-TCPP nanosheet/GO/GCE (c) at a current density of 10A/g. (C) GCD curves of Cu-TCPP nanosheet/GO/GCE at different current densities (1-20A/g). (D) Specific capacitances derived from the GCE curves at thecurrent density of 1-20 A/g.

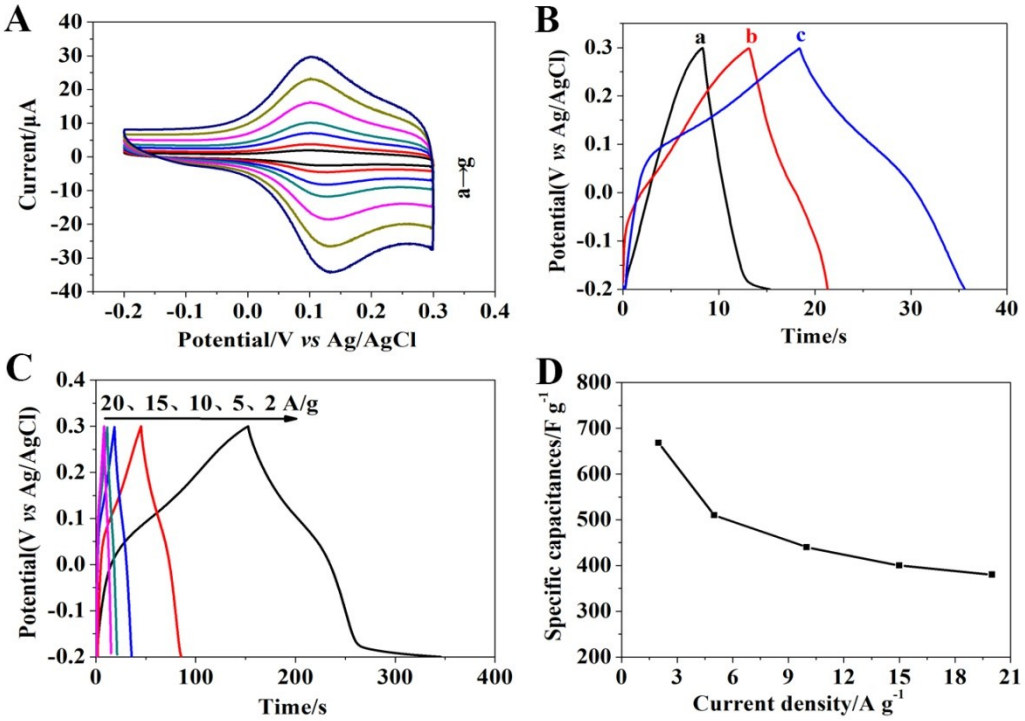

Figure S16. (A) CV curves of Co-TCPP nanosheet/GO/GCE at di□erent scan rates (a-g: 10-200 mV/s). (B) GCD curves of GO/GCE (a), Co-TCPP nanosheet/GCE (b) and Co-TCPP nanosheet/GO/GCE (c) at a current density of 10A/g. (C) GCD curves of Cu-TCPP nanosheet/GO/GCE at different current densities (2-20A/g). (D) Specific capacitances derived from the GCE curves at thecurrent density of 2-20 A/g.

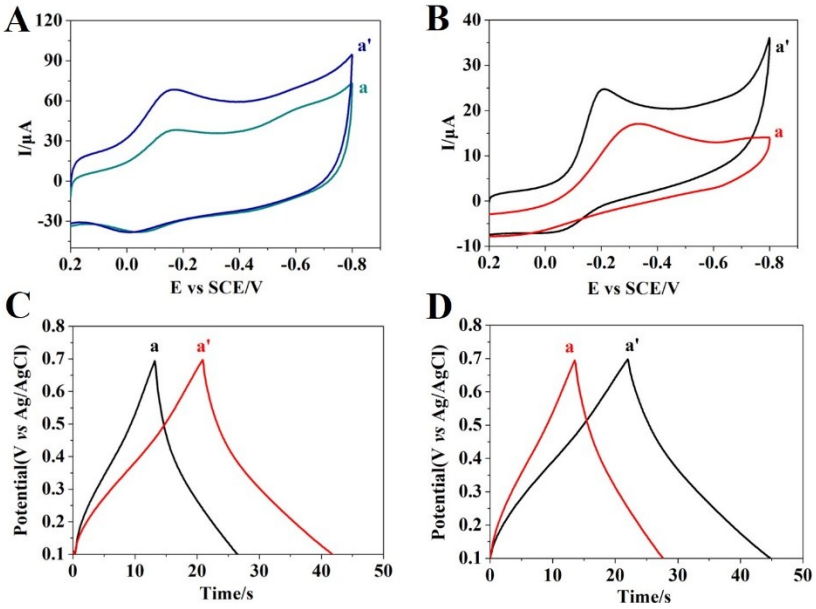

Figure S17. (A, B) CV curves of Cu-TCPP nanofilm+CNT/GCE (A, a), Cu-TCPP nanofilm/CNT/GCE (A, a'), Cu-TCPP nanosheet+GO/GCE (B, a), Cu-TCPP nanosheet/GO/GCE (B, b') in 0.1M PBS (pH 7.2) in presence of 0.2mM H_2O_2 at a scan rate of 50mV/s. (C, D) GCD curves of Cu-TCPP nanofilm+CNT/GCE (C, a), Cu-TCPP nanofilm/CNT/GCE (C, a'), Cu-TCPP nanosheet+GO/GCE (D, a), Cu-TCPP nanosheet/GO/GCE (D, a') at a current density of 10A/g.